Diffusion Models and Semi-Supervised Learners Benefit Mutually with Few Labels

Zebin You¹ Yong Zhong¹ Fan Bao² Jiacheng Sun³ Chongxuan Li¹ Jun Zhu²

Abstract

We propose a three-stage training strategy called dual pseudo training (DPT) for conditional image generation and classification in semi-supervised learning. First, a classifier is trained on partially labeled data and predicts pseudo labels for all data. Second, a conditional generative model is trained on all data with pseudo labels and generates pseudo images given labels. Finally, the classifier is trained on real data augmented by pseudo images with labels. We demonstrate largescale diffusion models and semi-supervised learners benefit mutually with a few labels via DPT. In particular, on the ImageNet 256×256 generation benchmark, DPT can generate realistic, diverse, and semantically correct images with very few labels. With two (i.e., < 0.2%) and five (i.e., <0.4%) labels per class, DPT achieves an FID of 3.44 and 3.37 respectively, outperforming strong diffusion models with full labels, such as IDDPM, CDM, ADM, and LDM. Besides, DPT outperforms competitive semi-supervised baselines substantially on ImageNet classification benchmarks with one, two, and five labels per class, achieving state-of-the-art top-1 accuracies of 59.0 (+2.8), 69.5 (+3.0), and 73.6 (+1.2) respectively.

1. Introduction

Classification and class-conditional generation are dual tasks that characterize opposite conditional distributions, e.g., p(label|image) and p(image|label). Learning such conditional distributions is conceptually natural given a sufficient amount of image-label pairs. Recent advances

Preprint.

in self-supervised learning¹ (He et al., 2020; Chen et al., 2020a; Chen & He, 2021; Grill et al., 2020; Xie et al., 2022; He et al., 2022a) and diffusion probabilistic models (Sohl-Dickstein et al., 2015; Ho et al., 2020; Song et al., 2021b; Dhariwal & Nichol, 2021; Bao et al., 2022a; Karras et al., 2022) achieve excellent performance in the two tasks respectively. However, both learning tasks are nontrivial in semi-supervised learning, where only a small fraction of the data are labeled (see Sec. 4 for a comprehensive review).

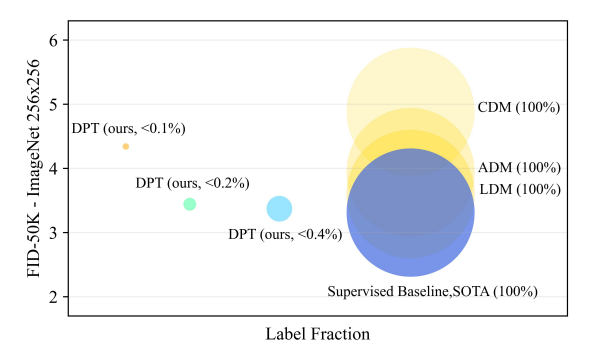
Most previous work solves the two tasks independently in semi-supervised learning while they can benefit mutually in intuition. The idea is best illustrated by a thought experiment with infinite model capacity and zero optimization error. Let p(image) be the true marginal distribution, from which we obtain massive samples in semi-supervised learning. Suppose we have a sub-optimal conditional distribution p_c (label|image) characterized by a classifier, a joint distribution $p_c(\text{image}, \text{label}) = p_c(\text{label}|\text{image})p(\text{image})$ is induced by predicting pseudo labels for unlabeled data. A conditional generative model trained on sufficient pseudo data from $p_c(\text{image}, \text{label})$ can induce the same joint distribution, as long as it is Fisher consistent² (Fisher, 1922). Because the generative model can further leverage the real data in a complementary way to the classifier, the induced joint distribution (denoted as p_a (image, label)) is probably closer to the true distribution than p_c (image, label). Similarly, the classifier can be enhanced by training on pseudo data sampled from p_q (image, label)). In conclusion, the classifier and the conditional generative model can benefit mutually through pseudo labels and data in the ideal case.

Inspired by the thought experiment, we propose a simple training strategy called *dual pseudo training* (DPT) for simultaneous image generation and classification in semi-supervised learning with very few labels (e.g., one label per class). DPT is three-staged (see Fig. 3). First, a classifier is trained on partially labeled data and used to predict pseudo labels for all data. Second, a conditional generative model is trained on all data with pseudo labels and used to gen-

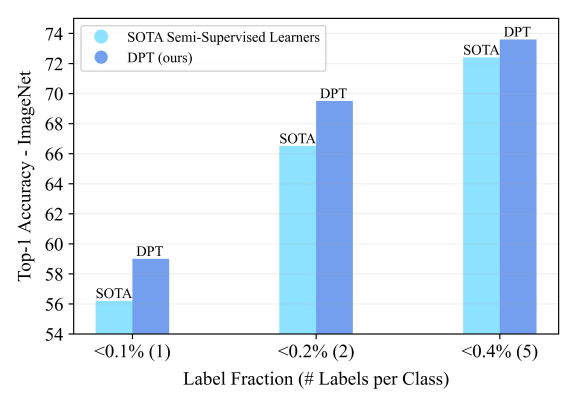
¹Gaoling School of AI, Renmin University of China; Beijing Key Laboratory of Big Data Management and Analysis Methods, Beijing, China ²Dept. of Comp. Sci. & Tech., Institute for AI, Tsinghua-Huawei Joint Center for AI, BNRist Center, State Key Lab for Intell. Tech. & Sys., Tsinghua University ³Huawei Noah's Ark Lab. Correspondence to: Chongxuan Li <chongxuanli@ruc.edu.cn>.

¹Self-supervised methods learn representations without labels but require full labels to obtain p(label|image).

²It means that the returned hypothesis in a sufficiently expressive class can recover the true distribution given infinite data.



(a) DPT with < 0.4% labels vs. supervised diffusion models.



(b) DPT vs. SOTA semi-supervised classifiers.

Figure 1. Generation and classification results of DPT on ImageNet with few labels. (a) DPT with < 0.4% labels outperforms strong supervised diffusion models (Dhariwal & Nichol, 2021; Ho et al., 2022; Rombach et al., 2022). The bubble area indicates the label fraction. (b) DPT substantially improves SOTA semi-supervised learners (Assran et al., 2022) with the same model.

erate pseudo images given labels. Finally, the classifier is trained on real data augmented by pseudo images with labels. Notably, we assume an infinite model capacity and zero optimization error in the above thought experiment. To reduce the gap between it and practice, we implement DPT based on large-scale vision transformers (ViT) (Dosovitskiy et al., 2021), strong self-supervised learners for semi-supervised learning (Assran et al., 2022), and diffusion probabilistic models (Ho et al., 2020; Bao et al., 2022a) with classifier-free guidance (Ho & Salimans, 2022).

We empirically demonstrate that large-scale diffusion probabilistic models and strong semi-supervised learners can benefit mutually with few labels via DPT (see Fig. 1). On the ImageNet 256×256 generation benchmark, DPT can generate realistic, diverse, and semantically correct images with very few labels (see Fig. 2). In particular, DPT with two (i.e., < 0.2%) labels per class is comparable to the state-of-the-art supervised baseline (Bao et al., 2022a) with the same architecture (FID 3.44 vs. 3.31). With *five* (i.e., < 0.4%) labels per class, DPT achieves an FID of 3.37, which

outperforms strong supervised diffusion models including IDDPM (Nichol & Dhariwal, 2021), CDM (Ho et al., 2022), ADM (Dhariwal & Nichol, 2021) and LDM (Rombach et al., 2022) (see Fig. 1 (a)). Besides, on ImageNet classification benchmarks with one, two, and five labels per class, DPT outperforms competitive semi-supervised baselines (Assran et al., 2022), achieving state-of-the-art top-1 accuracies of 59.0 (+2.8), 69.5 (+3.0), and 73.6 (+1.2) respectively (see Fig. 1 (b)). We also visualize and analyze the mutual effects between the classifier and the conditional generative model at the class level based on precision and recall, which explains the excellent performance of DPT.

2. Settings and Preliminaries

We present settings and preliminaries on a representative self-supervised learner for semi-supervised learning (Assran et al., 2022) in Sec. 2.1 and conditional diffusion probabilistic models (Ho et al., 2020; Bao et al., 2022a; Ho & Salimans, 2022) in Sec. 2.2, respectively.

We consider image generation and classification in semi-supervised learning, where the training set consists of N labeled images $\mathcal{S} = \{(\mathbf{x}_i^l, y_i^l)\}_{i=1}^N$ and M unlabeled images $\mathcal{D} = \{\mathbf{x}_i^u\}_{i=1}^M$. We assume $N \ll M$. For convenience, we denote the set of all real images as $\mathcal{X} = \{\mathbf{x}_i^u\}_{i=1}^M \cup \{\mathbf{x}_i^l\}_{i=1}^N$, and the set of all possible classes as \mathcal{Y} .

2.1. Masked Siamese Networks

Masked Siamese Networks (MSN) (Assran et al., 2022) employ a ViT-based (Dosovitskiy et al., 2021) anchor encoder $f_{\theta}(\cdot)$ and a target encoder $f_{\overline{\theta}}(\cdot)$, where $\overline{\theta}$ is the exponential moving average (EMA) (Grill et al., 2020) of parameters θ . For a real image $\mathbf{x}_i \in \mathcal{X}, 1 \leq i \leq M+N$, MSN obtains H+1 random augmented images, denoted as $\mathbf{x}_{i,h}, 1 \leq h \leq H+1$. MSN applies a random mask or focal mask to first H augmented images and obtain mask $(\mathbf{x}_{i,h}), 1 \leq h \leq H$. MSN optimizes θ and a learnable prototypes matrix \mathbf{q} by the following objective function:

$$\frac{1}{H(M+N)} \sum_{i=1}^{M+N} \sum_{h=1}^{H} \text{CE}(\mathbf{p}_{i,h}, \mathbf{p}_{i,H+1}) - \lambda \mathbf{H}(\bar{\mathbf{p}}), \quad (1)$$

where CE and H are cross entropy and entropy, $\mathbf{p}_{i,h} = \operatorname{softmax}((f_{\boldsymbol{\theta}}(\operatorname{mask}(\mathbf{x}_{i,h})) \cdot \mathbf{q}/\tau)$, $\bar{\mathbf{p}}$ is the mean of $\mathbf{p}_{i,h}$, $\mathbf{p}_{i,H+1} = \operatorname{softmax}(f_{\bar{\boldsymbol{\theta}}}(\mathbf{x}_{i,H+1}) \cdot \mathbf{q}/\tau')$, τ,τ' and λ are hyper-parameters, and \cdot denotes cosine similarity.

Finally, MSN extracts features for all labeled images in \mathcal{S} and trains a linear classifier in a supervised manner on the top of the features for prediction.





(a) Random samples from DPT trained with one (< 0.1%) label per class. Left: "King penguin". Right: "Ostrich".





(b) Random samples from DPT trained with **two** (< **0.2**%) **labels per class** . *Left:* "Black swan". *Right:* "Lesser panda".





(c) Random samples from DPT trained with five (< 0.4%) labels per class. Left: "Indigo bunting". Right: "Flamingo".

Figure 2. Random samples from DPT. DPT can generate realistic, diverse, and semantically correct images with very few training labels.

2.2. Conditional Diffusion Probabilistic Models

Denoising Diffusion Probabilistic Model (DDPM) (Ho et al., 2020) gradually adds noise $\epsilon \sim \mathcal{N}(\mathbf{0}, \mathbf{I})$ to data \mathbf{x}_0 from time t=0 to t=T in the forward process, and progressively removes noise to recover data starting at $\mathbf{x}_T \sim \mathcal{N}(\mathbf{0}, \mathbf{I})$ in the reverse process. It trains a predictor ϵ_{θ} to predict the noise ϵ by the following objective:

$$\mathcal{L} = \mathbb{E}_{t,\mathbf{x}_0,\epsilon}[||\epsilon_{\theta}(\mathbf{x}_t,\mathbf{c},t) - \epsilon||_2^2], \tag{2}$$

where c indicates conditions such as classes and texts.

Classifier-Free Guidance (CFG) (Ho & Salimans, 2022) leverages a conditional noise predictor $\epsilon_{\theta}(\mathbf{x}_t, \mathbf{c}, t)$ and an unconditional noise predictor $\epsilon_{\theta}(\mathbf{x}_t, t)$ in inference to improve sample quality and enhance semantics. Formally, CFG iterates the following equation starting at \mathbf{x}_T :

$$\mathbf{x}_{t-1} = \frac{1}{\sqrt{\alpha_t}} (\mathbf{x}_t - \frac{\beta_t}{\sqrt{1 - \bar{\alpha}_t}} \tilde{\boldsymbol{\epsilon}}_t) + \sigma_t^2 \mathbf{z}, \tag{3}$$

where $\tilde{\epsilon}_t = (1 + \omega)\epsilon_{\theta}(\mathbf{x}_t, \mathbf{c}, t) - \omega\epsilon_{\theta}(\mathbf{x}_t, t)$, ω is the guidance strength, $\mathbf{z} \sim \mathcal{N}(\mathbf{0}, \mathbf{I})$, and α_t , β_t , $\bar{\alpha}_t$ and σ_t are constants w.r.t. the time t.

U-ViT (Bao et al., 2022a) is a ViT-based backbone for diffusion probabilistic models, which achieves excellent performance in conditional sampling on large-scale datasets.

3. Method

Inspired by the thought experiment in Sec. 1, we solve the conditional image generation and image classification tasks in semi-supervised learning simultaneously. In particular, we propose a three-stage strategy called *dual pseudo training (DPT)*, illustrated in Fig. 3 and detailed as follows.

First Stage: Train Classifier. DPT trains a semi-supervised classifier on partially labeled data $S \cup D$, predicts a pseudo label \hat{y} of any image $\mathbf{x} \in \mathcal{X}$ by the classifier, and constructs a dataset consisting of all images with pseudo

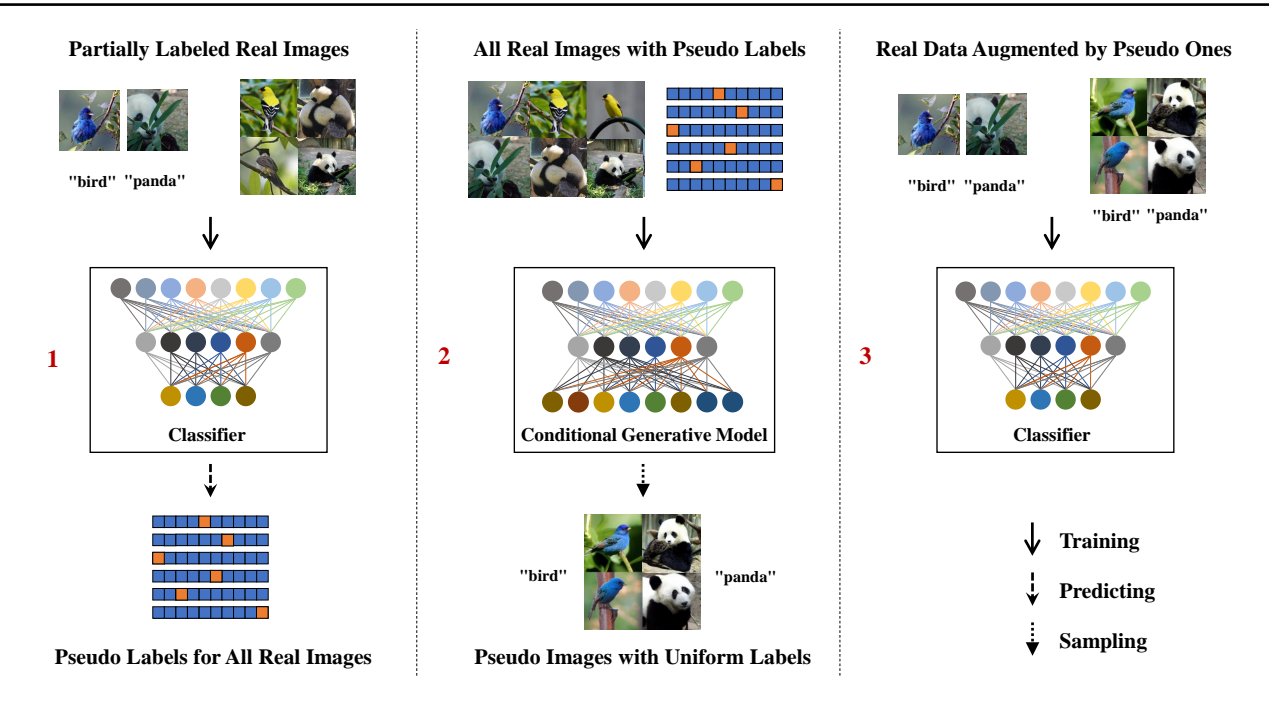


Figure 3. An overview of DPT. First, a (self-supervised) classifier is trained on partially labeled data and used to predict pseudo labels for all data. Second, a (diffusion-based) conditional generative model is trained on all data with pseudo labels and used to generate pseudo images given random labels. Finally, the classifier is trained or fine-tuned on real data augmented by pseudo images with labels.

labels, i.e. $S_1 = \{(\mathbf{x}, \hat{y}) | \mathbf{x} \in \mathcal{X}\}^3$. Notably, here we treat the classifier as a black box without modifying the training strategy or any hyperparameter. Therefore, any well-trained classifier can be adopted in DPT in a plug-and-play manner. Indeed, we exploit the recent advances in self-supervised learners for semi-supervised learning, i.e. MSN (Assran et al., 2022) with different ViT models, detailed in Sec. 2.1.

Second Stage: Classifier Benefits Generative Model. DPT trains a conditional generative model on all real images with pseudo labels \mathcal{S}_1 , samples K pseudo images for any class label y after training, and constructs a dataset consisting of pseudo images with uniform labels⁴. We denote the dataset as $\mathcal{S}_2 = \bigcup_{y \in \mathcal{Y}} \{(\hat{\mathbf{x}}_{i,y}, y)\}_{i=1}^K$, where $\hat{\mathbf{x}}_{i,y}$ is the i-th pseudo image for class y.

Similarly to the classifier, DPT also treats the conditional generative model as a black box. Inspired by the impressive image generation results of diffusion probabilistic models, we take a U-ViT-based (Bao et al., 2022a) denoise diffusion probabilistic model (Ho et al., 2020) with classifier-free guidance (Ho & Salimans, 2022) as the conditional generative model. Everything remains the same as the original work (See Sec. 2.2) except that the set of all real images with pseudo labels \mathcal{S}_1 is used for training.

We emphasize that S_1 obtained by the first stage is necessary. In fact, S is of small size (e.g., one label per class) and not sufficient to train conditional diffusion models. Besides, it is unclear how to leverage unlabeled data to train such models. Built upon strong semi-supervised approaches (Assran et al., 2022), S_1 provides useful learning signals (with relatively small noise) to train conditional diffusion models. DPT can generate realistic, diverse, and semantically correct images. We present quantitative and qualitative empirical evidence in Fig. 1 (a) and Fig. 2 respectively.

Third Stage: Generative Model Benefits Classifier. DPT trains the classifier employed in the first stage on real data augmented by S_2 to boost classification performance. For simplicity and efficiency, DPT freezes the models pretrained by Eq. (1) in the first stage and replaces S with $S \cup S_2$ to train a linear probe in MSN (Assran et al., 2022). All other settings remain the same. DPT substantially boosts the classification performance as presented in Fig. 1 (b). In principle, the augmented data can also be used in self-supervised pre-training, which is left as future work.

We can leverage the classifier in the third stage to refine the pseudo labels and train the generative model with one more stage. Although we observe an improvement empirically (see results in Appendix D.3), we focus on the three-stage strategy in the main paper for simplicity and efficiency.

³For simplicity, we also use pseudo labels instead of the ground-truth for real labeled data, which are rare and have a small zero-one training loss, making no significant difference.

⁴The prior distribution of y can be estimated on S.

4. Related Work

Semi-Supervised Classification and Generation. The two tasks are often studied independently. For semisupervised classification, classical work includes generative approaches based on VAE (Kingma et al., 2014; Maaløe et al., 2016; Li et al., 2017b) and GAN (Springenberg, 2016; Salimans et al., 2016; Dai et al., 2017; Gan et al., 2017; Li et al., 2021a; Zhang et al., 2021b), and discriminative approaches with confidence regularization (Joachims et al., 1999; Grandvalet & Bengio, 2004; Lee et al., 2013; Iscen et al., 2019) and consistency regularization (Miyato et al., 2018; Tarvainen & Valpola, 2017; Laine & Aila, 2017; Luo et al., 2018; Athiwaratkun et al., 2019; Oliver et al., 2018; Berthelot et al., 2019b;a; Li et al., 2021b; Zheng et al., 2022; Sohn et al., 2020; Zhang et al., 2021a; Assran et al., 2021). Recently, large-scale self-supervised approaches (Chen et al., 2020b; Grill et al., 2020; Cai et al., 2021; Assran et al., 2022; Cai et al., 2022) have made remarkable progress in semi-supervised learning.

Semi-supervised conditional image generation is challenging because generative modeling is more complex than prediction. In addition, it is highly nontrivial to design proper regularization when the input label is missing. Existing work is based on VAE (Kingma et al., 2014) or GAN (Li et al., 2017a; Lučić et al., 2019), which are limited to low-resolution data (i.e., $\leq 128 \times 128$) and require 10% labels or so to achieve comparable results to supervised baselines.

In comparison, DPT handles both classification and generation tasks in extreme settings with few labels (e.g., one label per class). Built upon recent advances in self-supervised learners and diffusion models, DPT substantially improves the state-of-the-art results in both tasks.

Pseudo Data and Labels. We mention additional work on generating pseudo data for contrastive representation learning (Jahanian et al., 2022) and zero-shot learning (He et al., 2022b; Besnier et al., 2020). Besides, prior work (Noroozi, 2020; Liu et al., 2020; Casanova et al., 2021; Bao et al., 2022b) uses cluster index or instance index as pseudo labels to improve unsupervised generation results, which are not directly comparable to DPT. With additional few labels, DPT can generate images of much higher quality and directly control the semantics of images with class labels.

Diffusion Models. Recently, diffusion probabilistic models (Springenberg, 2016; Ho et al., 2020; Song et al., 2021b; Karras et al., 2022) achieve remarkable progress in image generation (Dhariwal & Nichol, 2021; Rombach et al., 2022; Ho et al., 2022; Bao et al., 2022b; Ho & Salimans, 2022), text-to-image generation (Nichol et al., 2022; Ramesh et al., 2022; Gu et al., 2022; Rombach et al., 2022; Balaji et al., 2022), 3D scene generation (Poole et al., 2022), image-editing (Meng et al., 2022; Choi et al., 2021; Zhao et al.,

2022), and molecular design (Hoogeboom et al., 2022; Bao et al., 2022e). There are learning-free methods (Song et al., 2021a; Bao et al., 2022d; Lu et al., 2022a;b; Zhang & Chen, 2022) and learning-baed ones (Bao et al., 2022c; Salimans & Ho, 2022) to speed up the sampling process of diffusion models. In particular, we adopt third-order DPM-solver (Lu et al., 2022a), which is a recent learning-free method, for fast sampling. As for the architecture, most diffusion models rely on variants of the U-Net architecture introduced in score-based models (Song & Ermon, 2019) while recent work (Bao et al., 2022a) proposes a promising vision transformer for diffusion models, as employed in DPT.

To the best of our knowledge, there is little work on labelefficient conditional diffusion models and diffusion-based semi-supervised classification, as considered in this paper.

5. Experiment

We present the main experimental settings in Sec. 5.1. For more details, please refer to Appendix B. We compare DPT with state-of-the-art conditional diffusion models and semi-supervised learners in Sec. 5.2 and Sec. 5.3 respectively. We also visualize and analyze the interaction between the stages to explain the excellent performance of DPT.

5.1. Experimental Settings

Dataset. We evaluate DPT on the ImageNet (Deng et al., 2009) dataset, which consists of 1,281,167 training and 50,000 validation images. In the first and third stages, we use the same pre-processing protocol for real images as the baselines (Assran et al., 2022). For instance, in MSN, the real data are resized to 256×256 and then center-cropped to 224×224 . In the second stage, real images are center-cropped to a size of 256×256 following Bao et al. (2022a). In the third stage, the pseudo images are center-cropped to 224×224 . For semi-supervised classification, we consider the challenging settings with one, two, and five labels per class, and 1% labels. The labeled and unlabeled data split is the same as Assran et al. (2022).

Baselines. For semi-supervised classification, we reproduce the state-of-the-art self-supervised approach (Assran et al., 2022) with very few labels as the baseline. For conditional generation, we consider the state-of-the-art diffusion models with a U-ViT architecture (Bao et al., 2022a) as the baseline.

Model Architectures and Hyperparameters. For a fair comparison, we use exactly the same architectures and hyperparameters as the baselines (Assran et al., 2022; Bao et al., 2022a). In particular, we employ a ViT B/4 or a ViT L/7 model for classification and a U-ViT-Large model for conditional generation. We present more details in Appendix B. The only extra hyperparameter in DPT is the number of augmented pseudo images per class, i.e., *K*. We

Table 1. Image generation results on ImageNet 256×256. † labels the results taken from the corresponding references and * labels two baselines reproduced by us. DPT and both baselines employ exactly the same model architectures (Bao et al., 2022a). We present the gap of FID between DPT and the supervised baseline in parentheses. With < 0.4% labels, DPT outperforms strong conditional generative models with full labels, including CDM (Ho et al., 2022), ADM (Dhariwal & Nichol, 2021) and LDM (Rombach et al., 2022).

Method	Model	Label fraction (# labels/class)	FID-50K↓	sFID↓	IS ↑	Precision ↑	Recall ↑
BigGAN-deep (Brock et al., 2018) [†] StyleGAN-XL (Sauer et al., 2022) [†]	GAN GAN	100% 100%	6.95 2.30	7.36 4.02	171.4 265.12	0.87 0.78	0.28 0.53
ADM (Dhariwal & Nichol, 2021) [†] U-ViT (unsupervised baseline)*	Diff. Diff.	0% 0%	26.21 27.99	6.35 7.03	39.70 33.86	0.61 0.60	0.63 0.62
IDDPM (Nichol & Dhariwal, 2021) [†] CDM (Ho et al., 2022) [†] ADM (Dhariwal & Nichol, 2021) [†] LDM-4-G (Rombach et al., 2022) [†] U-ViT (Bao et al., 2022a) [†] U-ViT (supervised baseline)*	Diff. Diff. Diff. Diff. Diff. Diff. Diff.	100% 100% 100% 100% 100% 100%	12.26 4.88 3.94 3.60 3.40 3.31	5.42 - 6.14 - - 6.68	158.71 215.84 247.67 - 221.61	0.70 - 0.83 0.87 - 0.83	0.62 - 0.53 0.48 - 0.53
DPT (ours) with U-ViT and MSN L/7 DPT (ours) with U-ViT and MSN B/4	Diff. Diff.	< 0.1%(1) < 0.1%(1)	4.34 (1.03) 4.61 (1.30)	6.68 6.62	162.96 151.90	0.80 0.79	0.53 0.53
DPT (ours) with U-ViT and MSN L/7 DPT (ours) with U-ViT and MSN B/4	Diff. Diff.	< 0.2%(2) < 0.2%(2)	3.44 (0.13) 3.53 (0.22)	6.58 6.57	199.74 194.66	0.82 0.82	0.53 0.52
DPT (ours) with U-ViT and MSN L/7 DPT (ours) with U-ViT and MSN B/4	Diff. Diff.	< 0.4%(5) < 0.4%(5)	3.73 (0.42) 3.37 (0.06)	6.63 6.71	209.32 217.53	0.84 0.83	0.51 0.52
DPT (ours) with U-ViT and MSN L/7 DPT (ours) with U-ViT and MSN B/4	Diff. Diff.	$1\% (\approx 12) \\ 1\% (\approx 12)$	3.35 (0.04) 3.55 (0.24)	6.66 6.78	223.09 223.95	0.83 0.84	0.52 0.51

perform a simple grid search on $\{12, 128, 256, 512, 1280\}$ in MSN (ViT-L/7) with two labels per class and set K=128 as the default value if not specified.

Evaluation metrics. We use the top-1 accuracy on the validation set to evaluate classification performance. For a comprehensive evaluation of generation performance, we consider the Fréchet inception distance (FID) score (Heusel et al., 2017), sFID (Nash et al., 2021), Inception Score (IS) (Salimans et al., 2016), precision, and recall (Kynkäänniemi et al., 2019) on 50K generated samples. We calculate all generation metrics based on the official implementation of ADM (Dhariwal & Nichol, 2021).

Computational Cost. DPT shares exactly the same computational cost (\approx 4930 Nvidia V100 hours) to train the classifier and conditional generative model as the corresponding baselines in the first two stages. Additionally, DPT predicts pseudo labels for all data after the first stage and samples K=128 pseudo images per class after the second stage. DPT exploits the third-order DPM-solver (Lu et al., 2022a) with 50 steps for fast sampling. In the third stage, DPT reuses the model pre-trained in a self-supervised manner and only trains a linear classifier with pseudo images. Overall, DPT only introduces 1.32% (\approx 65 Nvidia V100 hours) extra computation. We present the detailed GPU hours in each stage in Appendix C.

Implementation. DPT is easy to understand and implement. In particular, it only requires several lines of code based on the implementation of the classifier and conditional diffusion model. We provide the pseudocode of DPT in the style of PyTorch in Appendix A.

5.2. Image Generation with Few Labels

Classifier Benefits Generation. Tab. 1 compares DPT with state-of-the-art generative models on the ImageNet 256×256 generation benchmark quantitatively. We construct very competitive baselines based on diffusion models with U-ViT (Bao et al., 2022a). According to Tab. 1, our supervised baseline achieves a state-of-the-art FID of 3.31 in diffusion models. Our unsupervised baseline achieves an FID of 27.99. DPT and both baselines employ exactly the same model architectures and hyperparameters. Leveraging the pseudo labels predicted by the strong semi-supervised learner (Assran et al., 2022), DPT with few labels improves the unconditional baseline significantly and is even comparable to the supervised baseline under all metrics. In particular, with only two labels per class, DPT improves the FID of the unsupervised baseline by 24.55 and is comparable to the supervised baseline with a gap of 0.13 (see the parentheses following the FID results of DPT in Tab. 1). Moreover, with five (i.e., < 0.4%) labels per class, DPT

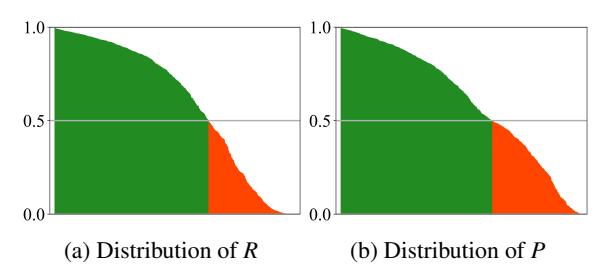


Figure 4. Distributions of R and P. The vertical axis represents the values of P and R w.r.t the classifier trained in the first stage. The horizontal axis represents all classes sorted by the values.



(a) *P* (0.99), *R* (1.00) (b) *P* (0.16), *R* (0.75) (c) *P* (0.99), *R* (0.23) "Giant Panda" "Purse" "Hornbill"

Figure 5. Random samples in selected classes with different P and R. (a) High P and R ensure good samples. (b) Low P leads to semantical confusion. (c) Low R lowers the visual quality.

achieves an FID of 3.37, outperforming strong supervised diffusion models including IDDPM (Nichol & Dhariwal, 2021), CDM (Ho et al., 2022), ADM (Dhariwal & Nichol, 2021) and LDM (Rombach et al., 2022).

Qualitatively, as presented in Fig. 2, DPT can generate realistic, diverse, and semantically correct images with very few labels, which agrees with the quantitative results in Tab. 1. We provide more samples and failure cases in Appendix D.1.

How Does Classifier Benefit Generation? We explain why the classifier can benefit the generative model through class-level visualization and analysis based on precision and recall on training data. For a given class y, the precision and recall w.r.t. the classifier is defined by $P = TP/(TP + FP)^5$ and R = TP/(TP + FN), where TP, FP, and FN denote the number of true positive, false positive, and false negative samples respectively. Intuitively, higher P and R suggest smaller noise in pseudo labels and result in better samples. Therefore, we employ strong semi-supervised learners (Assran et al., 2022) in the first stage to reduce the noise. In particular, with one label per class, MSN (Assran et al., 2022) with ViT-L/7 achieves a top-1 training accuracy of 60.3%. As presented in Fig. 4, R and P of most classes are higher than 0.5. Although noise exists, such a strong classifier can benefit the generative model overall.

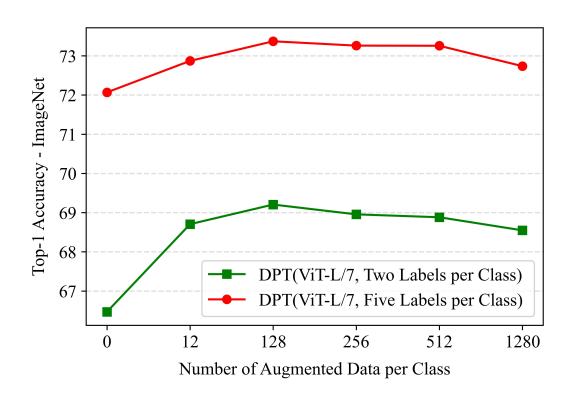


Figure 6. Sensitivity of K. DPT improves the baselines (K=0) with K in a large range. K=128 is the best choice.

We further select three representative classes with different values of P and R and visualize the samples in Fig. 5. In particular, the pseudo labels in a class with both high P and R contain little noise, leading to good samples (Fig. 5 (a)). In contrast, on one hand, a low P means that a large fraction of images labeled as y in S_1 are not actually in class y, and the samples from the generative model given the label y can be semantically wrong (Fig. 5 (b)). On the other hand, a low R means that a large fraction of images in class y are misclassified as other labels and the samples from the generative model can be less realistic due to the lack of training images in class y (Fig. 5 (c)).

5.3. Image Classification with Few Labels

Generative Model Benefits Classification. Tab. 2 compares DPT with state-of-the-art semi-supervised classifiers on the ImageNet validation set with few labels. DPT outperforms strong semi-supervised baselines (Assran et al., 2022) substantially with one, two, and five labels per class and achieves state-of-the-art top-1 accuracies of 59.0, 69.5, and 73.6, respectively. We present the improvement of DPT over the baseline in parentheses following the corresponding result of DPT. In particular, with two labels per class, DPT leverages the pseudo data generated by the diffusion model and improves MSN with ViT-B/4 by an accuracy of 4.6%. For completeness, we also report the results with 1% labels, the improvement is consistent yet marginal. We hypothesize that it is because the capability of the current diffusion models is limited. However, we believe DPT can be further improved with the development of diffusion models and this paper focuses on settings with very few labels (i.e. no more than five labels per class).

We further analyze the sensitivity of DPT w.r.t. K in Fig. 6 with two labels and five labels per class. We observe that K=128 is the best choice in both settings. According to Tab. 2, K=12 is better than K=128 with one label per class. Intuitively, the classifier will be dominated by

 $^{^{5}}$ We omit the dependence on y for simplicity.

Table 2. **Top-1 accuracy on the ImageNet validation set with few labels.** † labels the results taken from corresponding references, ‡ labels the results taken from Assran et al. (2022) and * labels the baselines reproduced by us. DPT and the corresponding baseline employ exactly the same classifier architectures. We present the gain of DPT over the corresponding baseline in parentheses. With one, two, five labels per class, DPT improves the state-of-the-art semi-supervised learner (Assran et al., 2022) consistently and substantially.

Method	Architecture	Top-1 accuracy ↑ given # labels per class (label fraction)				
		1(<0.1%)	2(<0.2%)	5(<0.5%)	$\approx 12(1\%)$	
EMAN (Cai et al., 2021) [†]	ResNet-50	-	-	-	63.0	
PAWS (Assran et al., 2021) [†]	ResNet-50	-	-	-	66.5	
BYOL (Grill et al., 2020) [†]	ResNet-200 (2 \times)	-	-	-	71.2	
SimCLR v2 (Chen et al., 2020b) [†]	ResNet-152 (3 \times)	-	-	-	76.6	
Semi-ViT (Cai et al., 2022) [†]	ViT-Huge	-	-	-	80.0	
iBOT (Zhou et al., 2022) [‡]	ViT-B/16	46.1 ± 0.3	56.2 ± 0.7	64.7 ± 0.3	-	
DINO (Caron et al., 2021) [‡]	ViT-B/8	45.8 ± 0.5	55.9 ± 0.6	64.6 ± 0.2	-	
MAE (He et al., 2022a) [‡]	ViT-L/16	12.3 ± 0.2	19.3 ± 1.8	42.3 ± 0.3	-	
MAE (He et al., 2022a) [‡]	ViT-H/14	11.6 ± 0.4	18.6 ± 0.2	32.8 ± 0.2	-	
MSN (Assran et al., 2022) [†]	ViT-B/4	54.3 ± 0.4	64.6 ± 0.7	72.4 ± 0.3	75.7	
MSN (Assran et al., 2022) [†]	ViT-L/7	57.1 ± 0.6	66.4 ± 0.6	72.1 ± 0.2	75.1	
MSN (baseline)*	ViT-B/4	52.9	64.9	72.4	75.3	
DPT (ours, $K = 12$)	ViT-B/4	58.2 (+5.3)	68.7 (+3.8)	73.2 (+0.8)	75.3 (+0.0)	
DPT (ours, K = 128)	ViT-B/4	58.6 (+5.7)	69.5 (+4.6)	73.6 (+1.2)	75.4 (+0.1)	
MSN (baseline)*	ViT-L/7	56.2	66.5	72.0	75.0	
DPT (ours, $K = 12$)	ViT-L/7	59.0 (+2.8)	68.7 (+2.2)	72.9 (+0.9)	75.2 (+0.2)	
DPT (ours, K = 128)	ViT-L/7	58.9 (+2.7)	69.2 (+2.7)	73.4 (+1.4)	75.3 (+0.3)	

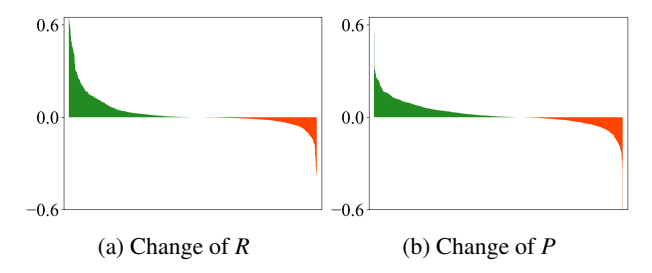


Figure 7. Distributions of the Change of *R* and *P*. The vertical axis represents the values of change after the third stage. The horizontal axis represents all classes sorted by the values of change.

the pseudo images and ignore real data with an overly large K, which explains the sub-optimal performance with K > 128. Nevertheless, according to Fig. 6, DPT improves the baselines (K = 0) consitently and substantially with K in a large range of $\{12, 128, 256, 512, 1280\}$.

How Does Generative Model Benefit Classification? Similarly to Sec. 5.2, we explain why the generative model can benefit the classifier through class-level visualization and analysis based on precision (P) and recall (R). After the third stage, we plot the distributions of the change of R and P in MSN (ViT-L/7) and one label per class in Fig 7. We can see a clear overall positive change of both R and P, indicating that the augmented dataset S_2 benefits the classifier.

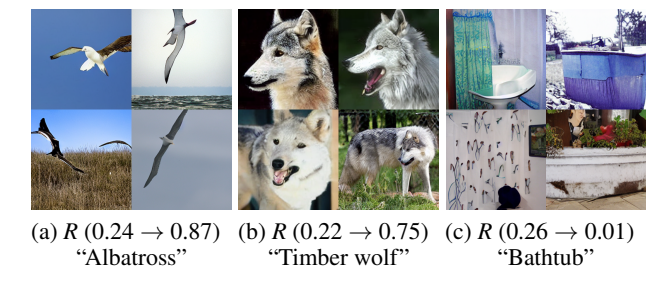


Figure 8. Random samples in selected classes with different values of change of *R*. Values of change are presented in parentheses. (a-b) If pseudo images are realistic and semantically correct, they can benefit classification. (c) Otherwise, they hurt performance.

We select three representative classes with different values of change of R for visualization in Fig. 8. If the pseudo images in class y are realistic, diverse, and semantically correct, then it can increase the corresponding R as presented in Fig. 8 (a-b). Instead, poor samples may hurt the classification performance in the corresponding class, as shown in Fig. 8 (c). The analysis of P involves pseudo images in multiple classes, which is presented in Appendix D.2.

6. Conlusion

This paper presents a training strategy DPT for conditional image generation and classification in semi-supervised learn-

- ing. DPT is simple to implement and achieves excellent performance in both tasks on ImageNet. DPT probably inspires future work in semi-supervised learning.
- **Social Impact:** We believe that DPT can benefit real-world applications with few labels (e.g., medical analysis). However, the proposed label-efficient diffusion models may aggravate social issues such as "DeepFakes". The problem can be relieved by automatic detection with machine learning, which is an active research area.

References

- Assran, M., Caron, M., Misra, I., Bojanowski, P., Joulin, A., Ballas, N., and Rabbat, M. Semi-supervised learning of visual features by non-parametrically predicting view assignments with support samples. In *Proceedings of the IEEE/CVF International Conference on Computer Vision*, pp. 8443–8452, 2021.
- Assran, M., Caron, M., Misra, I., Bojanowski, P., Bordes, F., Vincent, P., Joulin, A., Rabbat, M., and Ballas, N. Masked siamese networks for label-efficient learning. In *European Conference on Computer Vision*, pp. 456–473. Springer, 2022.
- Athiwaratkun, B., Finzi, M., Izmailov, P., and Wilson, A. G. There are many consistent explanations of unlabeled data: Why you should average. In 7th International Conference on Learning Representations, ICLR 2019, New Orleans, LA, USA, May 6-9, 2019, 2019.
- Balaji, Y., Nah, S., Huang, X., Vahdat, A., Song, J., Kreis, K., Aittala, M., Aila, T., Laine, S., Catanzaro, B., et al. ediffi: Text-to-image diffusion models with an ensemble of expert denoisers. *arXiv preprint arXiv:2211.01324*, 2022.
- Bao, F., Li, C., Cao, Y., and Zhu, J. All are worth words: a vit backbone for score-based diffusion models. *arXiv* preprint arXiv:2209.12152, 2022a.
- Bao, F., Li, C., Sun, J., and Zhu, J. Why are conditional generative models better than unconditional ones? In *NeurIPS 2022 Workshop on Score-Based Methods*, 2022b.
- Bao, F., Li, C., Sun, J., Zhu, J., and Zhang, B. Estimating the optimal covariance with imperfect mean in diffusion probabilistic models. In *Proceedings of the 39th International Conference on Machine Learning*, pp. 1555–1584, 2022c.
- Bao, F., Li, C., Zhu, J., and Zhang, B. Analytic-dpm: an analytic estimate of the optimal reverse variance in diffusion probabilistic models. In *The Tenth International Conference on Learning Representations, ICLR 2022, Virtual Event, April 25-29, 2022*, 2022d.

- Bao, F., Zhao, M., Hao, Z., Li, P., Li, C., and Zhu, J. Equivariant energy-guided sde for inverse molecular design. *arXiv* preprint arXiv:2209.15408, 2022e.
- Berthelot, D., Carlini, N., Cubuk, E. D., Kurakin, A., Sohn, K., Zhang, H., and Raffel, C. Remixmatch: Semi-supervised learning with distribution matching and augmentation anchoring. In *International Conference on Learning Representations*, 2019a.
- Berthelot, D., Carlini, N., Goodfellow, I., Papernot, N., Oliver, A., and Raffel, C. A. Mixmatch: A holistic approach to semi-supervised learning. In *Advances in Neural Information Processing Systems*, pp. 5049–5059, 2019b.
- Besnier, V., Jain, H., Bursuc, A., Cord, M., and Pérez, P. This dataset does not exist: training models from generated images. In *ICASSP 2020-2020 IEEE International Conference on Acoustics, Speech and Signal Processing (ICASSP)*, pp. 1–5. IEEE, 2020.
- Brock, A., Donahue, J., and Simonyan, K. Large scale gan training for high fidelity natural image synthesis. In *International Conference on Learning Representations*, 2018.
- Cai, Z., Ravichandran, A., Maji, S., Fowlkes, C., Tu, Z., and Soatto, S. Exponential moving average normalization for self-supervised and semi-supervised learning. In *Proceedings of the IEEE/CVF Conference on Computer Vision and Pattern Recognition*, pp. 194–203, 2021.
- Cai, Z., Ravichandran, A., Favaro, P., Wang, M., Modolo, D., Bhotika, R., Tu, Z., and Soatto, S. Semi-supervised vision transformers at scale. In *NeurIPS*, 2022.
- Caron, M., Touvron, H., Misra, I., Jégou, H., Mairal, J., Bojanowski, P., and Joulin, A. Emerging properties in self-supervised vision transformers. In *Proceedings of* the *IEEE/CVF International Conference on Computer* Vision, pp. 9650–9660, 2021.
- Casanova, A., Careil, M., Verbeek, J., Drozdzal, M., and Romero Soriano, A. Instance-conditioned gan. *Advances* in Neural Information Processing Systems, 34:27517– 27529, 2021.
- Chen, T., Kornblith, S., Norouzi, M., and Hinton, G. E. A simple framework for contrastive learning of visual representations. In *International Conference on Machine Learning*, volume 119, pp. 1597–1607, 2020a.
- Chen, T., Kornblith, S., Swersky, K., Norouzi, M., and Hinton, G. E. Big self-supervised models are strong semi-supervised learners. *Advances in neural information processing systems*, 33:22243–22255, 2020b.

- Chen, X. and He, K. Exploring simple siamese representation learning. In *IEEE Conference on Computer Vision and Pattern Recognition*, pp. 15750–15758, 2021.
- Choi, J., Kim, S., Jeong, Y., Gwon, Y., and Yoon, S. Ilvr: Conditioning method for denoising diffusion probabilistic models. In 2021 IEEE/CVF International Conference on Computer Vision (ICCV), pp. 14347–14356, 2021.
- Dai, Z., Yang, Z., Yang, F., Cohen, W. W., and Salakhutdinov, R. R. Good semi-supervised learning that requires a bad gan. In *Advances in Neural Information Processing Systems*, pp. 6510–6520, 2017.
- Deng, J., Dong, W., Socher, R., Li, L., Li, K., and Fei-Fei, L. Imagenet: A large-scale hierarchical image database. In IEEE Computer Society Conference on Computer Vision and Pattern Recognition, pp. 248–255, 2009.
- Dhariwal, P. and Nichol, A. Diffusion models beat gans on image synthesis. *Advances in Neural Information Processing Systems*, 34:8780–8794, 2021.
- Dosovitskiy, A., Beyer, L., Kolesnikov, A., Weissenborn,
 D., Zhai, X., Unterthiner, T., Dehghani, M., Minderer,
 M., Heigold, G., Gelly, S., Uszkoreit, J., and Houlsby, N.
 An image is worth 16x16 words: Transformers for image recognition at scale. In 9th International Conference on Learning Representations, ICLR 2021, Virtual Event, Austria, May 3-7, 2021, 2021.
- Fisher, R. A. On the mathematical foundations of theoretical statistics. *Philosophical transactions of the Royal Society of London. Series A, containing papers of a mathematical or physical character*, 222(594-604):309–368, 1922.
- Gan, Z., Chen, L., Wang, W., Pu, Y., Zhang, Y., Liu, H., Li, C., and Carin, L. Triangle generative adversarial networks. In *Advances in Neural Information Processing Systems*, pp. 5247–5256, 2017.
- Grandvalet, Y. and Bengio, Y. Semi-supervised learning by entropy minimization. In *Advances in Neural Information Processing Systems*, volume 17, 01 2004.
- Grill, J.-B., Strub, F., Altché, F., Tallec, C., Richemond, P., Buchatskaya, E., Doersch, C., Avila Pires, B., Guo, Z., Gheshlaghi Azar, M., et al. Bootstrap your own latent-a new approach to self-supervised learning. *Advances in neural information processing systems*, 33:21271–21284, 2020.
- Gu, S., Chen, D., Bao, J., Wen, F., Zhang, B., Chen, D., Yuan, L., and Guo, B. Vector quantized diffusion model for text-to-image synthesis. In *Proceedings of the IEEE/CVF Conference on Computer Vision and Pattern Recognition*, pp. 10696–10706, 2022.

- He, K., Fan, H., Wu, Y., Xie, S., and Girshick, R. B. Momentum contrast for unsupervised visual representation learning. In *IEEE/CVF Conference on Computer Vision and Pattern Recognition*, pp. 9726–9735, 2020.
- He, K., Chen, X., Xie, S., Li, Y., Dollár, P., and Girshick, R. B. Masked autoencoders are scalable vision learners. In *IEEE/CVF Conference on Computer Vision and Pattern Recognition*, pp. 15979–15988, 2022a.
- He, R., Sun, S., Yu, X., Xue, C., Zhang, W., Torr, P., Bai, S., and Qi, X. Is synthetic data from generative models ready for image recognition? *arXiv preprint arXiv:2210.07574*, 2022b.
- Heusel, M., Ramsauer, H., Unterthiner, T., Nessler, B., and Hochreiter, S. Gans trained by a two time-scale update rule converge to a local nash equilibrium. In *Advances in Neural Information Processing Systems*, pp. 6626–6637, 2017.
- Ho, J. and Salimans, T. Classifier-free diffusion guidance. *arXiv preprint arXiv:2207.12598*, 2022.
- Ho, J., Jain, A., and Abbeel, P. Denoising diffusion probabilistic models. In *Advances in Neural Information Processing Systems*, 2020.
- Ho, J., Saharia, C., Chan, W., Fleet, D. J., Norouzi, M., and Salimans, T. Cascaded diffusion models for high fidelity image generation. *J. Mach. Learn. Res.*, 23:47–1, 2022.
- Hoogeboom, E., Satorras, V. G., Vignac, C., and Welling, M. Equivariant diffusion for molecule generation in 3d. In *International Conference on Machine Learning*, pp. 8867–8887. PMLR, 2022.
- Iscen, A., Tolias, G., Avrithis, Y., and Chum, O. Label propagation for deep semi-supervised learning. In *Proceedings of the IEEE conference on computer vision and pattern recognition*, pp. 5070–5079, 2019.
- Jahanian, A., Puig, X., Tian, Y., and Isola, P. Generative models as a data source for multiview representation learning. In *The Tenth International Conference on Learning Representations, ICLR 2022, Virtual Event, April 25-29*, 2022, 2022.
- Joachims, T. et al. Transductive inference for text classification using support vector machines. In *ICML*, volume 99, pp. 200–209, 1999.
- Karras, T., Aittala, M., Aila, T., and Laine, S. Elucidating the design space of diffusion-based generative models. In *Proc. NeurIPS*, 2022.
- Kingma, D. P., Mohamed, S., Rezende, D. J., and Welling, M. Semi-supervised learning with deep generative models. In Advances in Neural Information Processing Systems, 2014.

- Kynkäänniemi, T., Karras, T., Laine, S., Lehtinen, J., and Aila, T. Improved precision and recall metric for assessing generative models. *Advances in Neural Information Processing Systems*, 32, 2019.
- Laine, S. and Aila, T. Temporal ensembling for semisupervised learning. In *International Conference on Learning Representations*, 2017.
- Lee, D.-H. et al. Pseudo-label: The simple and efficient semi-supervised learning method for deep neural networks. In *Workshop on challenges in representation learning, ICML*, volume 3, pp. 896, 2013.
- Li, C., Xu, K., Zhu, J., and Zhang, B. Triple generative adversarial nets. In *Advances in Neural Information Processing Systems*, pp. 4088–4098, 2017a.
- Li, C., Zhu, J., and Zhang, B. Max-margin deep generative models for (semi-) supervised learning. *IEEE transactions on pattern analysis and machine intelligence*, 40 (11):2762–2775, 2017b.
- Li, C., Xu, K., Zhu, J., Liu, J., and Zhang, B. Triple generative adversarial networks. *IEEE Transactions on Pattern Analysis and Machine Intelligence*, 2021a.
- Li, J., Xiong, C., and Hoi, S. C. Comatch: Semi-supervised learning with contrastive graph regularization. In *Proceedings of the IEEE/CVF International Conference on Computer Vision*, pp. 9475–9484, 2021b.
- Liu, S., Wang, T., Bau, D., Zhu, J.-Y., and Torralba, A. Diverse image generation via self-conditioned gans. In *Proceedings of the IEEE/CVF conference on computer vision and pattern recognition*, pp. 14286–14295, 2020.
- Lu, C., Zhou, Y., Bao, F., Chen, J., Li, C., and Zhu, J. Dpm-solver: A fast ode solver for diffusion probabilistic model sampling in around 10 steps. *arXiv* preprint *arXiv*:2206.00927, 2022a.
- Lu, C., Zhou, Y., Bao, F., Chen, J., Li, C., and Zhu, J. Dpm-solver++: Fast solver for guided sampling of diffusion probabilistic models. *arXiv preprint arXiv:2211.01095*, 2022b.
- Lučić, M., Tschannen, M., Ritter, M., Zhai, X., Bachem, O., and Gelly, S. High-fidelity image generation with fewer labels. In *International conference on machine learning*, pp. 4183–4192. PMLR, 2019.
- Luo, Y., Zhu, J., Li, M., Ren, Y., and Zhang, B. Smooth neighbors on teacher graphs for semi-supervised learning. In *Proceedings of the IEEE conference on computer vision and pattern recognition*, pp. 8896–8905, 2018.

- Maaløe, L., Sønderby, C. K., Sønderby, S. K., and Winther, O. Auxiliary deep generative models. In *International* conference on machine learning, pp. 1445–1453. PMLR, 2016.
- Mairal, J. Cyanure: An open-source toolbox for empirical risk minimization for python, c++, and soon more. *arXiv* preprint arXiv:1912.08165, 2019.
- Meng, C., He, Y., Song, Y., Song, J., Wu, J., Zhu, J., and Ermon, S. Sdedit: Guided image synthesis and editing with stochastic differential equations. In *The Tenth International Conference on Learning Representations, ICLR* 2022, Virtual Event, April 25-29, 2022, 2022.
- Miyato, T., Maeda, S.-i., Koyama, M., and Ishii, S. Virtual adversarial training: a regularization method for supervised and semi-supervised learning. *IEEE transactions on pattern analysis and machine intelligence*, 41(8):1979–1993, 2018.
- Nash, C., Menick, J., Dieleman, S., and Battaglia, P. W. Generating images with sparse representations. In *Proceedings of the 38th International Conference on Machine Learning, ICML 2021, 18-24 July 2021, Virtual Event*, volume 139, pp. 7958–7968, 2021.
- Nichol, A. Q. and Dhariwal, P. Improved denoising diffusion probabilistic models. In *International Conference on Machine Learning*, pp. 8162–8171. PMLR, 2021.
- Nichol, A. Q., Dhariwal, P., Ramesh, A., Shyam, P., Mishkin, P., McGrew, B., Sutskever, I., and Chen, M. GLIDE: towards photorealistic image generation and editing with text-guided diffusion models. In *International Conference on Machine Learning, ICML 2022, 17-23 July 2022, Baltimore, Maryland, USA*, volume 162, pp. 16784–16804, 2022.
- Noroozi, M. Self-labeled conditional gans. *arXiv* preprint *arXiv*:2012.02162, 2020.
- Oliver, A., Odena, A., Raffel, C. A., Cubuk, E. D., and Goodfellow, I. Realistic evaluation of deep semi-supervised learning algorithms. In *Advances in Neural Information Processing Systems*, pp. 3235–3246, 2018.
- Poole, B., Jain, A., Barron, J. T., and Mildenhall, B. Dreamfusion: Text-to-3d using 2d diffusion. *arXiv* preprint *arXiv*:2209.14988, 2022.
- Ramesh, A., Dhariwal, P., Nichol, A., Chu, C., and Chen, M. Hierarchical text-conditional image generation with clip latents. *arXiv preprint arXiv:2204.06125*, 2022.
- Rombach, R., Blattmann, A., Lorenz, D., Esser, P., and Ommer, B. High-resolution image synthesis with latent

- diffusion models. In *Proceedings of the IEEE/CVF Conference on Computer Vision and Pattern Recognition*, pp. 10684–10695, 2022.
- Salimans, T. and Ho, J. Progressive distillation for fast sampling of diffusion models. In *The Tenth International Conference on Learning Representations, ICLR 2022, Virtual Event, April 25-29, 2022, 2022.*
- Salimans, T., Goodfellow, I., Zaremba, W., Cheung, V., Radford, A., and Chen, X. Improved techniques for training GANs. In *Advances in Neural Information Processing Systems*, 2016.
- Sauer, A., Schwarz, K., and Geiger, A. Stylegan-xl: Scaling stylegan to large diverse datasets. In *ACM SIGGRAPH* 2022 Conference Proceedings, pp. 1–10, 2022.
- Sohl-Dickstein, J., Weiss, E. A., Maheswaranathan, N., and Ganguli, S. Deep unsupervised learning using nonequilibrium thermodynamics. In *Proceedings of the 32nd International Conference on Machine Learning*, 2015.
- Sohn, K., Berthelot, D., Carlini, N., Zhang, Z., Zhang, H., Raffel, C. A., Cubuk, E. D., Kurakin, A., and Li, C.-L. Fixmatch: Simplifying semi-supervised learning with consistency and confidence. *Advances in neural informa*tion processing systems, 33:596–608, 2020.
- Song, J., Meng, C., and Ermon, S. Denoising diffusion implicit models. In 9th International Conference on Learning Representations, ICLR 2021, Virtual Event, Austria, May 3-7, 2021, 2021a.
- Song, Y. and Ermon, S. Generative modeling by estimating gradients of the data distribution. *Advances in Neural Information Processing Systems*, 32, 2019.
- Song, Y., Sohl-Dickstein, J., Kingma, D. P., Kumar, A., Ermon, S., and Poole, B. Score-based generative modeling through stochastic differential equations. In 9th International Conference on Learning Representations, 2021b.
- Springenberg, J. T. Unsupervised and semi-supervised learning with categorical generative adversarial networks. In Bengio, Y. and LeCun, Y. (eds.), 4th International Conference on Learning Representations, ICLR 2016, San Juan, Puerto Rico, May 2-4, 2016, Conference Track Proceedings, 2016.
- Tarvainen, A. and Valpola, H. Mean teachers are better role models: Weight-averaged consistency targets improve semi-supervised deep learning results. In *Advances in Neural Information Processing Systems*, pp. 1195–1204, 2017.

- Xie, Z., Zhang, Z., Cao, Y., Lin, Y., Bao, J., Yao, Z., Dai, Q., and Hu, H. Simmim: A simple framework for masked image modeling. In *International Conference on Computer Vision and Pattern Recognition (CVPR)*, 2022.
- Zhang, B., Wang, Y., Hou, W., Wu, H., Wang, J., Okumura, M., and Shinozaki, T. Flexmatch: Boosting semi-supervised learning with curriculum pseudo labeling. *Advances in Neural Information Processing Systems*, 34: 18408–18419, 2021a.
- Zhang, Q. and Chen, Y. Fast sampling of diffusion models with exponential integrator. In *NeurIPS 2022 Workshop on Score-Based Methods*, 2022.
- Zhang, Y., Ling, H., Gao, J., Yin, K., Lafleche, J.-F., Barriuso, A., Torralba, A., and Fidler, S. Datasetgan: Efficient labeled data factory with minimal human effort. In Proceedings of the IEEE/CVF Conference on Computer Vision and Pattern Recognition, pp. 10145–10155, 2021b.
- Zhao, M., Bao, F., Li, C., and Zhu, J. Egsde: Unpaired image-to-image translation via energy-guided stochastic differential equations. Advances in Neural Information Processing Systems, 2022.
- Zheng, M., You, S., Huang, L., Wang, F., Qian, C., and Xu, C. Simmatch: Semi-supervised learning with similarity matching. In *Proceedings of the IEEE/CVF Conference on Computer Vision and Pattern Recognition*, pp. 14471–14481, 2022.
- Zhou, J., Wei, C., Wang, H., Shen, W., Xie, C., Yuille, A., and Kong, T. ibot: Image bert pre-training with online tokenizer. *International Conference on Learning Representations (ICLR)*, 2022.

Algorithm 1 Pseudocode of DPT in a PyTorch style.

```
MSN: a feature extractor in the self-supervised setting
  LinearClassifier: a linear classifier UViT: a conditional diffusion model real_labeled_data: real labeled data
  real_unlabeled data: real unlabeled data
all_real_images: all images in real labeled and unlabeled data
C: the number of classes in real labeled and unlabeled data
  K: the number of pseudo samples
# Uniform: uniform sampling function
## first stage
MSN.train(all_real_images) # train a self-supervised learner
real_labeled_data_features = MSN.extract(real_labeled_data.images) # extract features of images in labeled data
LinearClassifier.train([(real_labeled_data_features, real_labeled_data.labels)]) # train a classifer
pseudo_labels = LinearClassifier.predict(all_real_images) # predict labels for all real images
## second stage
UViT.train([(all_real_images, pseudo_labels)]) # train a conditional diffusion model
uniform_labels = Uniform(C, K) # uniformly sample K labels from [0, C)
pseudo_images = UViT.sample(uniform_labels) # sample K pseudo images by UViT
## third stage
pseudo_images_features = MSN.extract(pseudo_images) # extract features of pseudo images
LinearClassifier.train([(real_labeled_data_features,real_labeled_data.labels),
                             (pseudo_images_features, uniform_labels)]) # re-train the classifier
```

Table 3. The code links and licenses.

Method	Link	License
ADM	https://github.com/openai/guided-diffusion	MIT License
LDM	https://github.com/CompVis/latent-diffusion	MIT License
U-ViT	https://github.com/baofff/U-ViT	MIT License
DPM-Solver	https://github.com/LuChengTHU/dpm-solver	MIT License
MSN	https://github.com/facebookresearch/msn	CC BY-NC 4.0

Table 4. Model architectures in MSN and U-ViT.

Model	Param	# Layers	Hidden Size	MLP Size	# Heads
Semi-Supervised Classifier (MSN) ViT B/4 ViT L/7	86M 304M	12 24	768 1024	3072 4096	12 16
Conditional Diffusion Model (U-ViT) U-ViT-Large	287M	21	1024	4096	16

A. Pseudocode of DPT

Algorithm 1 presents the pseudocode of DPT in the PyTorch style. Based on the implementation of the classifier and the conditional generative model, DPT is easy to implement with a few lines of code in PyTorch.

B. Experimental Setting

We implement DPT upon the official code of LDM, DPM-Solver, ADM, MSN and U-ViT, whose code links and licenses are presented in Tab. 3. After the double-blind review, we will release our source code. All the architectures and hyperparameters



Figure 9. An overview of computation in DPT. DPT introduces a little extra computation, as indicated by blue blocks.

are the same as the corresponding baselines (Bao et al., 2022a; Assran et al., 2022). For completeness, we briefly mention important settings and refer the readers to the original paper for more details.

Network architectures. We present the network architectures in Tab. 4.

MSN pre-training. MSN adopts a warm-up strategy over the first 15 epochs of training, which linearly increases the learning rate from 0.0002 to 0.001, and then decays the learning rate to 0 following a cosine schedule. The total training epochs are 200 and 300 for the architecture of ViT L/7 and ViT B/4, separately. The batch size is 1024 for both two architectures.

Linear Classifier. After extracting the features by MSN, we use the cyanure package (Mairal, 2019) to train the classifier following MSN (Assran et al., 2022). In particular, we run logistic regression on a single CPU core based on cyanure.

U-ViT. U-ViT is based on the latent diffusion (Rombach et al., 2022) for ImageNet 256×256 generation. It trains a transformer-based conditional generative model with a batch size of 1024, a training iteration of 300k, and a learning rate of 2e-4.

C. Computational Cost

Fig. 9 presents the detailed computing cost of DPT. Training the classifier and conditional generative model is exactly the same as the baselines. For predicting pseudo labels, sampling pseudo images, and training the linear classifier in the third stage, DPT introduces 1.32% additional computation cost approximately, which is negligible.

D. Additional Results

D.1. More Samples and Failure Cases

Fig. 10 shows more random samples generated by DPT, which are natural, diverse, and semantically consistent with the corresponding classes.

Moreover, Fig. 11 depicts the randomly generated images in selected classes, from DPT trained with one, two, and five real labels per class. As shown in Fig. 11 (a), if the classifier can make accurate predictions given one label per class, then DPT can generate images of high quality. However, we found failure cases of DPT in Fig. 11 (d) and (g), where the samples are of incorrect semantics due to the large noise in the pseudo labels. Nevertheless, as the number of labels increases, the generation performance of DPT becomes better due to more accurate predictions.

Notably, in Fig. 11, we fix the same random seed for image generation in the same class across DPT with a different number of labels (e.g., Fig. 11 (a-c)) for a fair and clear comparison. The samples of different models given the same random seed are similar because all models attempt to characterize the same diffusion ODE and the discretization of the ODE does not introduce extra noise (Lu et al., 2022a), as observed in existing diffusion models (Song et al., 2021b; Bao et al., 2022a).

D.2. Analysis of Change of Precision in the Third Stage

According to the definition of precision (i.e. P = TP/(TP + FP)), the pseudo images can affect P through not only TP but also FP. We select two representative classes with positive change of P to visualize both cases, as shown in Fig. 12. We select top-three classes according to the number of images classified as "throne" and present the numbers w.r.t. the classifier after the first and third stages in Fig. 12 (a) and (b) respectively. As shown in Fig. 12 (c), high-quality samples in the class "throne" directly increases TP (i.e., the number of images in class "throne" classified as "throne") and improves P. We





(a) Random samples with one label per class. Left: "Gondola". Right: "Yellow lady's slipper".





(b) Random samples with two labels per class. Left: "Triceratops". Right: "Echidna".





(c) Random samples with five labels per class. Left: "School bus". Right: "Fig".

Figure 10. More random samples in specific classes from DPT.

also present the top-three classes related to "four poster" in Fig. 12 (d) and (e). It can be seen that P in class "four poster" increases because of FP (of class "quilt" especially) decreases. We visulize random samples in both "four poster" and "quilt" in Fig. 12 (f). These high quality samples help the classifier to distinguish the two classes, which explains the change of FP and P. A similar analysis can be conducted for classes with negative change of P.

We mention that we analyze the change of P and R in the third stage on the training set instead of the validation set. This is because the training set is of much larger size and therefore leads to a much smaller variance in the estimate of P and R. Since most of the data are unlabeled in the training set, this does not introduce a large bias in the esimtate of P and R.

D.3. Results with More Stages

According to Tab. 2, we find that using generative augmentation can lead to more accurate predictions on unlabeled images. Therefore, we attempt to add a further stage employing the refined classifier to predict pseudo labels for all data, and then re-train the conditional generative model on them. As shown in Tab. 5, these refined pseudo labels indeed bring a consistent improvement on all quantitative metrics, showing promising promotion of more-stage training. However, note that re-training the conditional generative model is time-consuming and we focus on the three-stage strategy in this paper for simplicity and efficiency.

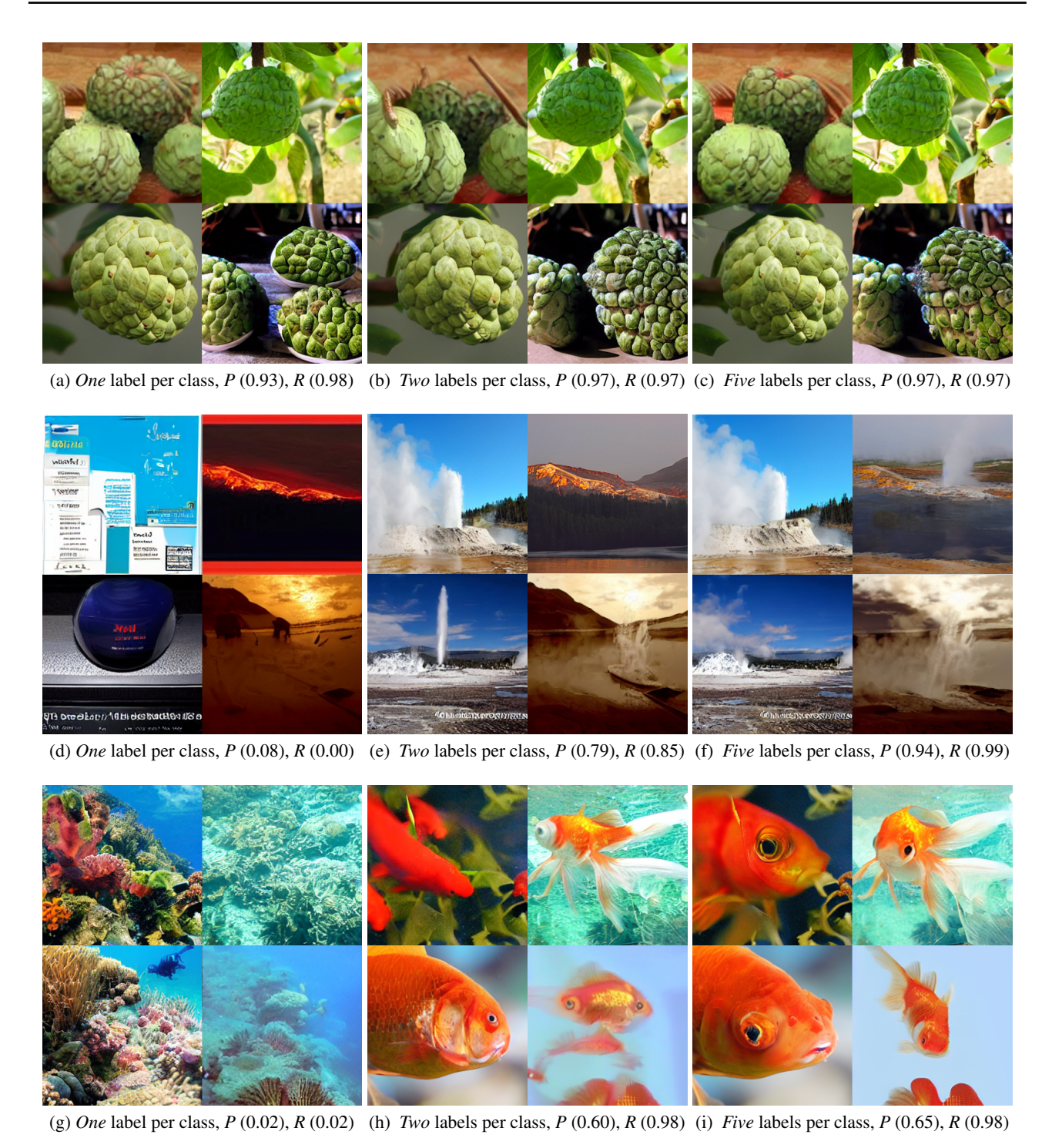


Figure 11. Random samples by varying the number of real labels in the first stage. More real labels result in smaller noise in pseudo labels and samples of better visual quality and correct semantics. *Top:* "Custard apple". *Middle:* "Geyser". *Bottom:* "Goldfish".

Table 5. **Effect of refined pseudo labels.** Results on ImageNet 256×256 benchmark with one label per class.

Method	FID↓	sFID↓	IS ↑	Precision ↑	Recall ↑
DPT DPT with refined pseudo labels	4.34	6.68	162.96	0.80	0.53
	4.00	6.56	178.05	0.81	0.53

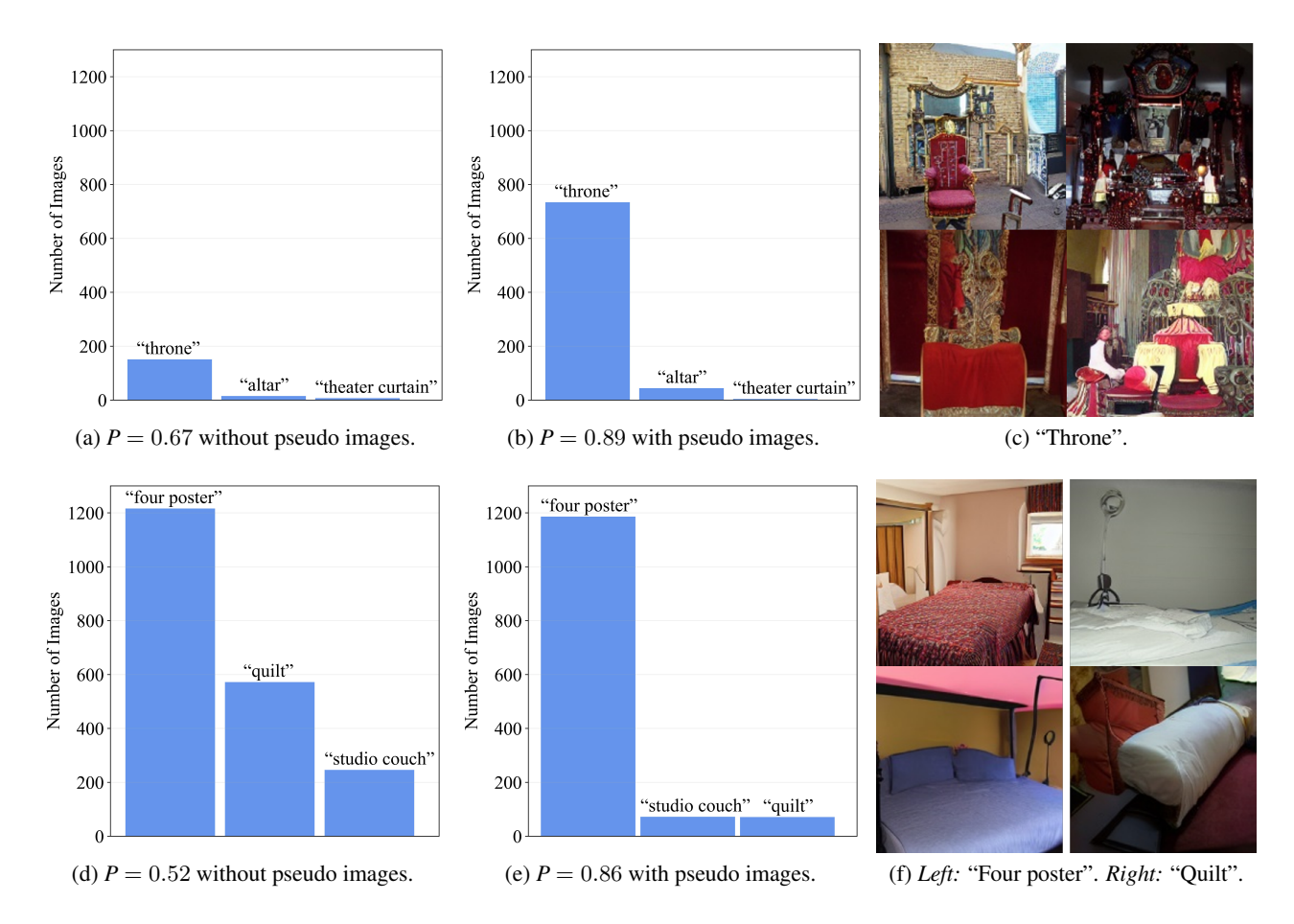


Figure 12. Detailed analysis in selected classes with a positive change of P. Top: "Throne". High-quality samples in the class "throne" (c) directly increases TP and improves P (a-b). Bottom: "Four poster". The samples in both "four poster" and "quilt" are of high quality (f). The classifier reduces FP with such pseudo samples and improves P (d-e).